Registry No. Poly(L-lysine) hydrobromide (homopolymer), 56148-61-9; poly(L-lysine) hydrobromide (SRU), 26588-20-5.

References and Notes

(1) Daniel, E.; Alexandrowicz, Z. *Biopolymers* **1963**, *1*, 473.
(2) Alexandrowicz, Z.; Daniel, E. *Biopolymers* **1963**, *1*, 447.
(3) Lee, W. I.; Schurr, J. M. *J. Polym. Sci., Polym. Phys. Ed.* **1975**, *13*, 873.
(4) Lin, S.-C.; Lee, W. I.; Schurr, J. M. *Biopolymers* **1978**, *17*, 1041.
(5) Ise, N.; Okubo, T. *Acc. Chem. Res.* **1980**, *13*, 303.
(6) Ise, N.; Okubo, T.; Sugimura, M.; Ito, K.; Nolte, H. J. *J. Chem. Phys.* **1983**, *78*, 536.
(7) Ise, N.; Okubo, T.; Yamamoto, K.; Matsuoka, H.; Kawai, H.; Hashimoto, T.; Fujimura, M. *J. Chem. Phys.* **1983**, *78*, 541.
(8) Nemoto, N.; Tsunashima, Y.; Kurata, M. *Polym. J.* **1981**, *13*, 827.
(9) Han. C. C.; Akcasu, A. Z. *Macromolecules* **1981**, *14*, 1080.
(10) See, for example: Oosawa, F. "Polyelectrolytes"; Marcel Dekker: New York, 1971.
(11) Kedem, O.; Katchalsky, A. *J. Polym. Sci.* **1955**, *15*, 321.
(12) Schurr, J. M. *J. Phys. Chem.* **1969**, *73*, 2820.

Soliton Model for Dielectric Relaxation in Crystalline Polyethylene. Comparison with Experiment

James L. Skinner* and Y. H. Park

Department of Chemistry, Columbia University, New York, New York 10027.
Received December 21, 1983

ABSTRACT: The Brownian soliton model for dielectric relaxation in crystalline polyethylene previously introduced by Skinner and Wolynes is used to analyze recent constant-volume experiments by Sayre et al. The non-Debye frequency dependence of the experimental susceptibility is fit extremely well by the theory. From our analysis we determine the temperature dependence of the soliton density. This leads to a value of the soliton energy that is in excellent agreement with an independent theoretical calculation. We speculate about the nature of soliton scattering in this system.

1. Introduction

Dielectric relaxation is a powerful method for probing molecular motion in condensed phases. In this paper we will be concerned with the orientational dynamics of polymer subunits in crystalline polyethylene. (Polyethylene is rendered dielectrically active by dilute oxidation.[1]) Since molecular reorientation is thermally activated, it is desirable to perform experiments at different temperatures. However, in general the volume of the sample is temperature dependent, and activation barriers are sensitive functions of volume. This entanglement of temperature and density effects complicates the analysis of experimental data. Recently, however, with the use of high-pressure techniques, a beautiful set of *constant-volume* experiments[1] have been performed that circumvent the above-mentioned problem.

The experiments on crystalline polyethylene show several relaxation processes, the slowest of which is known as the α-relaxation. This relaxation peak has been analyzed by fitting the frequency-dependent susceptibility to the empirical Cole–Cole equation,[2] finding, for example, that the width parameter is quite temperature dependent. In addition, the temperature dependence of the frequency of maximum loss is analyzed with absolute rate theory, giving the free energy of activation. While these approaches are useful in quantifying experimental data, they do not provide an unambiguous molecular mechanism for the relaxation process.

Although various molecular mechanisms for the α-relaxation process have been proposed (see the excellent discussion in ref 3), the most likely candidate was identified by Mansfield and Boyd.[3] They studied the energetics of defects in crystalline polyethylene with a potential energy surface discussed earlier by Boyd.[4] In particular, they discovered a mobile, localized defect with a creation energy of 18 kcal/mol. The defect is a 180° twist of an all-trans chain localized over about 12 CH_2 units. They found that about half of the creation energy resulted from the twisted region, while the other half stemmed from the translational mismatch of the chain ends. Furthermore, they found that the energy barrier to propagation of the twist was negligible, resulting in its high mobility. The passage of one of these mobile defects past a site with a dipole would cause dielectric relaxation by producing a 180° flip of the dipole.

Independently, Mansfield[5] and Skinner and Wolynes[6] recognized that this defect had the properties of a solitary wave and might well be modeled by soliton theory.[7] Mansfield[5] constructed a model with a rotational and translational degree of freedom for each CH_2 unit and concluded that the resulting equations of motion had solitary wave solutions. Skinner and Wolynes[6] (SW) considered only rotational degrees of freedom and described the system with the familiar sine–Gordon theory. While the latter approach is cruder than Mansfield's (because SW neglected translational degrees of freedom), it is in some ways more attractive because of its analytical tractability.

The frequency-dependent susceptibility is related through linear response theory to the dipole–dipole correlation function.[8] SW calculated the soliton contribution to this correlation function, finding exponential decay. This produces a Debye semicircle in the Cole–Cole plot, in disagreement with experiment. Thus, SW were prompted to consider the interactions of solitons with intrachain phonons or a thermal bath. On the basis of work of others,[9-11] SW proposed that the solutions undergo Brownian motion and calculated the resulting correlation function.

The purpose of this paper is to perform a detailed comparison of experiment[1] with the theory of SW. In section 2, we describe the theory of SW in some detail. In section 3, we fit the frequency-dependent data[1] for different temperatures, and we analyze the temperature dependence of the resulting parameters. We also speculate about the nature of soliton scattering in this system.

2. Soliton Model

From molecular mechanics modeling, Mansfield and Boyd[3] (MB) discovered the existence of a new kind of

0024-9297/84/2217-1735$01.50/0

localized topological defect in crystalline polyethylene. The defect consists of a gradual 180° twist of a polyethylene chain. About half of the energy of the defect arises from the twisted region, while the remainder results from the translational mismatch of the chain ends. These defects also have the property that propagation proceeds with a negligible barrier. Skinner and Wolynes[6] (SW) recognized that these defects are very similar, especially in the topological sense, to the solitons of a sine–Gordon model with period π. Thus, they constructed a model with a single rotational degree of freedom, θ_i, for each CH_2 group. The Hamiltonian of the SW model has the form

$$H = \sum_{i=1}^{N}\left\{A(1 - \cos(2\theta_i)) + \frac{I}{2}\dot{\theta}_i^2 + \frac{C}{2}(\theta_i - \theta_{i+1})^2\right\} \quad (1)$$

where N is the number of CH_2 units. The first term represents the crystal field potential that affects the motion of each CH_2 group. The second term is the total kinetic energy; I is the moment of inertia associated with each CH_2 group. The last term is the harmonic coupling between nearest-neighbor CH_2 groups.

As mentioned earlier, this Hamiltonian neglects translational degrees of freedom which, strictly speaking, are necessary for a complete description of polyethylene dynamics. Nonetheless, as we will see below, it is primarily the *topological* aspects (rather than the details) of the solitons that lead to the predicted theoretical correlation function. Thus, this oversimplified model is very useful in elucidating the nature of dielectric relaxation in crystalline polyethylene.

According to MB, the twist defect is delocalized over 12 CH_2 groups, so a continuum approximation is appropriate.[6] Thus, we let $\theta_i \rightarrow \theta(x)$ and

$$H = \int_{-L/2}^{L/2}\frac{dx}{l}\left\{A(1 - \cos(2\theta)) + \frac{I}{2}\dot{\theta}^2 + \frac{Cl^2}{2}\theta_x^2\right\} \quad (2)$$

where $\theta_x = \partial\theta/\partial x$, l is the distance between CH_2 groups, and $L = Nl$. The equation of motion for θ is[6]

$$\frac{\partial^2\theta}{\partial t^2} - c_0^2\frac{\partial^2\theta}{\partial x^2} + \frac{\omega_0^2}{2}\sin(2\theta) = 0 \quad (3)$$

$$c_0^2 = Cl^2/I \quad (4)$$

and

$$\omega_0^2 = 4A/I \quad (5)$$

The above is a sine–Gordon equation with period π. The soliton (antisoliton) solutions are

$$\theta_{s(\bar{s})}(x - x_0 - vt) = 2\arctan\left[\exp\left(\pm\frac{x - x_0 - vt}{\alpha(1 - v^2/c_0^2)^{1/2}}\right)\right] \quad (6)$$

where $\alpha = c_0/\omega_0$ and v is the soliton velocity ($v < c_0$).

Dielectric relaxation experiments measure the equilibrium dipole–dipole correlation function, $\Phi(t)$.[8] For dilute dipoles, the cross terms between individual molecular dipoles vanish, and within the context of the SW model[6]

$$\Phi(t) = \langle\cos(\theta(x,t) - \theta(x,0))\rangle \quad (7)$$

This correlation function has contributions from both phonons and solitons. However, to study the α-relaxation, only the slowest processes need be considered, and thus SW neglected the phonon contributions to $\Phi(t)$. They treated the system as a nonrelativistic ($v \ll c_0$) gas of noninteracting solitons and antisolitons. Furthermore, they assumed that due to interactions with other thermal excitations, the solitons performed Brownian motion. In the limit of low soliton density, SW found that

$$\theta(t) = \exp\left[-\frac{B}{\gamma}(\gamma t - 1 + e^{-\gamma t})^{1/2}\right] \quad (8)$$

where

$$B = 4n_0/(\beta m^*\pi)^{1/2} \quad (9)$$

$$\gamma = \zeta/m^* \quad (10)$$

In the above n_0 is the equilibrium soliton/antisoliton density, ζ is the friction constant for soliton motion, γ^{-1} is the soliton velocity correlation time, m^* is the effective soliton mass, and $\beta = 1/kT$. n_0 and m^* are expressed in terms of the model parameters as[6]

$$n_0 = \frac{4\omega_0}{c_0}\left(\frac{\beta E_s}{2\pi}\right)^{1/2}e^{-\beta E_s} \quad (11)$$

$$E_s = 2I\omega_0 c_0/l \quad (12)$$

$$m^* = E_s/c_0^2 \quad (13)$$

where E_s is the soliton energy.

When eq 11 and 13 are substituted into eq 9, we obtain

$$B = \frac{8(2^{1/2})}{\pi}\omega_0 e^{-E_s/kT} \quad (14)$$

It is extremely important to emphasize that the principal result embodied in eq 8–10 is somewhat more general than the sine–Gordon model from which it was derived. The *crucial* assumptions behind the derivation are as follows: (1) there exist localized defects with 180° twist topology, (2) the defects are very dilute so they can be taken as noninteracting, (3) the defects are mobile in the sense that there is no energy barrier to propagation, and (4) due to the interactions of the defects with the surroundings, they undergo classical Brownian motion. As discussed earlier, the defects of MB (which we will henceforth call solitons) satisfy assumptions 1 and 3. Because of the high creation energy compared to kT, the equilibrium soliton density should be very small and hence assumption 2 is satisfied. Thus, the only untested assumption for these defects is that they obey Brownian motion. If they do, the theoretically predicted correlation function is eq 8, with (9) and (10).

For the sine–Gordon solitons, the density and mass can be expressed in terms of microscopic parameters (eq 11–14). However, for the more general MB solitons we do not have corresponding microscopic expressions. Nonetheless, one would expect the equilibrium soliton density, n_0, to be proportional to $e^{-E_s/kT}$, where E_s is the soliton energy. Thus eq 9 becomes

$$B = B_0 e^{-E_s/kT} \quad (15)$$

where B_0 might contain a weak temperature dependence. For the most part, in what follows we will adopt this more general interpretation of eq 3 with (15) and will use the experimental data to determine E_s and the temperature dependence of γ. It will however be useful to refer to the microscopic expressions, eq 11–14 for the sine–Gordon model, in order to estimate several quantities such as the soliton diffusion constant.

Dielectric relaxation experiments measure the frequency-dependent complex dielectric constant, $\epsilon^*(\omega) = \epsilon'(\omega)$

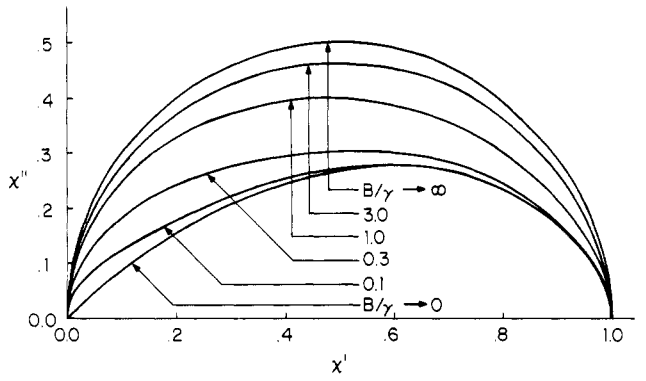

Figure 1. Theoretical Cole–Cole plots that result from the Brownian soliton model for various values of the ratio B/γ.

$-i\epsilon''(\omega)$, which is related to the dipole–dipole correlation function, $\Phi(t)$, by[8]

$$\chi^*(\omega) = \frac{\epsilon^*(\omega) - \epsilon_\infty}{\epsilon_0 - \epsilon_\infty} = -\int_0^\infty dt\, e^{-i\omega t} \frac{d\Phi(t)}{dt} \quad (16)$$

where ϵ_0 and ϵ_∞ are the limiting low- and high-frequency dielectric constants. Experimental data are often presented as a Cole–Cole plot: χ'' vs. χ', where $\chi^*(\omega) = \chi'(\omega) - i\chi''(\omega)$. Equation 8 leads to the following limiting cases. When $B/\gamma \gg 1$, $\Phi(t)$ becomes exponential

$$\Phi(t) \sim e^{-t/\tau} \quad (17)$$

with $\tau = 2^{1/2}/B$. Thus we have

$$\chi^*(\omega) = 1/(1 + i\omega\tau) \quad (18)$$

which gives the Debye semicircle in Figure 1. Alternatively, when $B/\gamma \ll 1$

$$\Phi(t) \sim e^{-(t/\tau)^{1/2}} \quad (19)$$

with $\tau = \gamma/B^2$. In this case[12]

$$\chi^*(\omega) = (1 - i)\left(\frac{\pi}{8\omega\tau}\right)^{1/2} W(z) \quad (20)$$

$$z = (1 + i)/(8\omega\tau)^{1/2}$$

$$W(z) = e^{-z^2}\,\mathrm{erfc}\,(-iz)$$

This limit is also shown in Figure 1 ($W(z)$ is tabulated in Ambramowitz and Stegun[13]). The result is very reminiscent of the Cole–Davidson skewed arc.[14,15] For other values of B/γ, the integral has been performed numerically and is shown in Figure 1. Thus we see that different values of the ratio B/γ give strikingly different Cole–Cole plots, varying from the Debye result to behavior resembling the Cole–Cole circular arc of the Cole–Davidson skewed arc.

The above limits correspond to the following physical situations. Since the thermal solution velocity is $v = (kT/m^*)^{1/2}$, from eq 9 we see that $B \sim vn_0$. n_0 is the inverse of the distance between solutions, so vn_0 is the inverse of the time it takes the nearest soliton to pass a given point in the absence of friction. On the other hand, γ is the soliton velocity relaxation rate. When $B \gg \gamma$, a soliton arrives at a dipole before its velocity is changed; i.e., it behaves as a free particle. When $\gamma \gg B$, the soliton's velocity correlation has been lost many times before it arrives; i.e., it diffuses.

3. Comparison with Experiment

The experimental data[1,16] consist of the real and imaginary frequency-dependent dielectric constants $\epsilon'(\omega)$ and $\epsilon''(\omega)$ for various temperatures and pressures. The pressures were chosen to allow measurements at different temperatures but at constant volume. We have analyzed

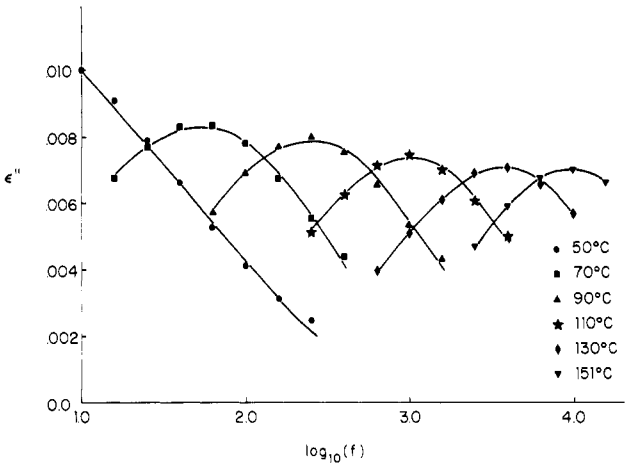

Figure 2. Imaginary part of the dielectric constant, ϵ'', as a function of frequency $f = \omega/2\pi$. The experimental points at different temperatures are represented by the various symbols, and the solid lines are the best theoretical fits from eq 21.

Table I
Best Fit Parameters B, γ, and $\epsilon_0 - \epsilon_\infty$ Obtained from Experimental Measurements[1] of $\epsilon''(\omega)$ at Different Temperatures and Pressures

specific vol, cm³/g	T, °C	press, kbar	B, s⁻¹	γ, s⁻¹	$\epsilon_0 - \epsilon_\infty$	B/γ
1.012	50	1.61	4.13	468	0.00615	0.0882
	70	2.08	349	994	0.00268	0.351
	90	2.45	1320	2340	0.00229	0.563
	110	2.88	4620	6700	0.00206	0.689
	130	3.36	17000	24200	0.00196	0.701
	151	4.12	35900	41700	0.00182	0.860
1.022	50	0.99	108	864	0.00476	0.125
	70	1.38	701	1420	0.00243	0.494
	90	1.77	2970	4800	0.00218	0.618
	110	2.11	11100	14400	0.00194	0.770
	130	2.56	39500	47300	0.00182	0.835
	151	3.17	97800	89700	0.00170	1.09
1.032	50	0.54	237	997	0.00335	0.238
	70	0.83	1430	2910	0.00234	0.491
	90	1.18	6020	9270	0.00208	0.649
	110	1.48	23800	27800	0.00182	0.857
	130	1.83	97900	106000	0.00174	0.924

data at three different volumes. Since $\epsilon'(\omega)$ and $\epsilon''(\omega)$ are related by the Kramers–Kronig expressions and are therefore not independent, we have fitted only $\epsilon''(\omega)$. Integrating eq 16 by parts and substituting in eq 8 for $\Phi(t)$, we obtain

$$\epsilon''(\omega) = (\epsilon_0 - \epsilon_\infty)\omega \int_0^\infty dt \cos(\omega t) \exp[-(B/\gamma) \times (\gamma t - 1 + \exp(-\gamma t))^{1/2}] \quad (21)$$

The parameters B, γ, and $\epsilon_0 - \epsilon_\infty$ were determined by a nonlinear least-squares fit[17] of the experimental data. This procedure was complicated by the fact that for each value of the parameters, the time integral in eq 21 had to be performed numerically. The experimental data and the theoretical fit for specific volume 1.022 cm³/g and different temperatures are shown in Figure 2. The agreement between the data and the fit is excellent. The best fit parameters for all three volumes are shown in Table I. Of immediate interest are the values of B/γ; they fall between about 0.1 and 1. According to Figure 1, this implies very non-Debye relaxation behavior. In particular, $B/\gamma \approx 1$ resembles a Cole–Cole circular arc, while $B/\gamma \approx 0.1$ resembles a Cole–Davidson skewed arc.

Although all the important microscopic information can be determined from ϵ'' alone, for illustrative purposes we

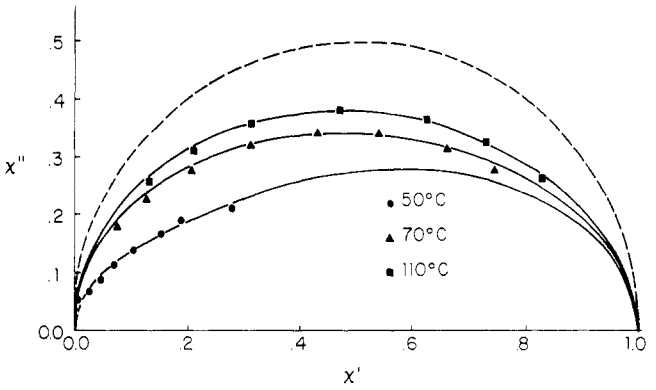

Figure 3. Cole–Cole plot of the experimental data at different temperatures for specific volume 1.022 cm^3/g. The solid lines are the best theoretical fits. For comparison, the Debye semicircle is shown by the dotted line.

Table II
Best Fit Parameters E_s and B_0 (or ω_0) Obtained from Analyzing the Parameter B from Table I with Eq 15 (or Eq 14) (See Figure 4)

specific vol, cm^3/g	E_s, kcal/mol	B_0, s^{-1}	ω_0, s^{-1}
1.012	18.2	1.0×10^{14}	2.9×10^{13}
1.022	18.4	3.4×10^{14}	9.5×10^{13}
1.032	19.3	2.5×10^{15}	6.8×10^{14}

have presented several sets of data in the Cole–Cole form, which involves both ϵ'' and ϵ'. From eq 16, we find that

$$\epsilon'(\omega) = \epsilon_\infty + (\epsilon_0 - \epsilon_\infty)\left\{1 - \omega \int_0^\infty dt \sin(\omega t) \exp[-(B/\gamma) \times (\gamma t - 1 + \exp(-\gamma t))^{1/2}]\right\} \quad (22)$$

For each temperature and pressure, the parameters B, γ, and $\epsilon_0 - \epsilon_\infty$ previously determined from $\epsilon''(\omega)$ were used. Thus the $\epsilon'(\omega)$ data was fit with a single adjustable parameter ϵ_∞. For the specific volume of 1.022 cm^3/g and several values of the temperature, the results are shown in Figure 3. As before, the agreement between theory and experiment is very satisfactory.

According to eq 14 or 15, B is proporational to $e^{-E_s/kT}$. Therefore, from a plot of ln (B) vs. $1/T$, we can obtain the soliton energy E_s and the parameter B_0 (or the frequency ω_0). Such a plot is shown in Figure 4 for the three different volumes. Also shown in each case is the best fit; all the data fall nicely on straight lines. The best fit parameters are shown in Table II. The difference between the parameters for different volumes is probably not significant, especially for ω_0 or B_0, since these values are obtained from large extrapolation. Of primary interest is the comparison of the soliton energy determined above of 18–19 kcal/mol with the soliton energy from the modeling calculations of MB. For crystals thicker than about 150 Å, MB found a twist defect energy of 18 kcal/mol, in excellent agreement with the values determined above.

The SW theory does not make an explicit prediction of the temperature dependence of γ, the soliton velocity relaxation rate. To discuss its temperature dependence, we note that γ can be related to the diffusion constant through the Einstein relation $D = kT/\zeta = kT/\gamma m^*$. Wada and Ishiuchi[10] considered the nonlinear interaction between solitons and intrachain phonons and found that $D \sim T^2$. For a related soliton-bearing Hamiltonian, the Φ^4 model, Wada and Schrieffer[10] found $D \sim T^2$, while Sahni and Mazenko[11] found $D \sim T^{1/2}$. These temperature dependences give $\gamma \sim T^{-1}$ and $\gamma \sim T^{1/2}$, predicting respectively that γ decreases or increases weakly with temperature.

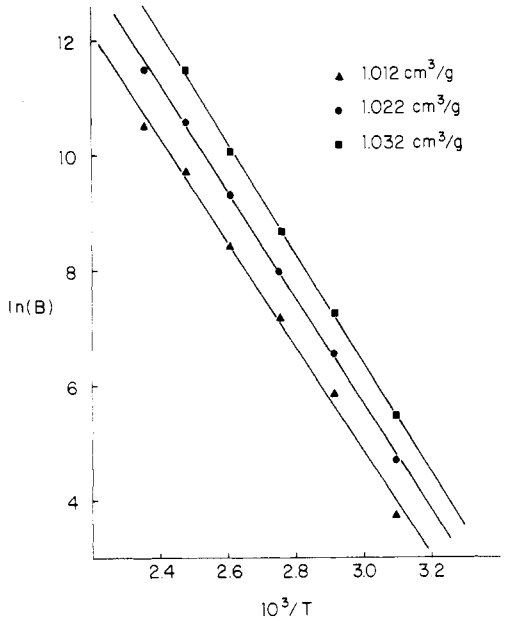

Figure 4. Temperature dependence of the parameter B from Table I for different specific volumes. The solid lines show the best fit to the Arrhenius form of eq 14 or 15. The resulting parameters are given in Table II.

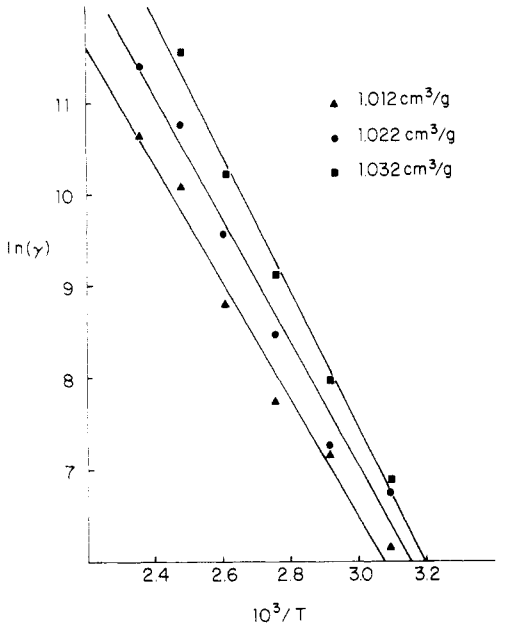

Figure 5. Temperature dependence of the parameter γ from Table I for different specific volumes. The solid lines show the best fit to the Arrhenius form of eq 23. The resulting parameters are given in Table III.

The data in Table I show that γ increases very rapidly with temperature (much faster than $T^{1/2}$). Thus we must conclude that the above mechanism is not important in these experiments. Because of the strong temperature dependence of γ displayed by Table I, we might assume an Arrhenius from (possible physical reasons for this are discussed below):

$$\gamma = \gamma_0 e^{-E_0/kT} \quad (23)$$

In Figure 5, we show a plot of ln (γ) vs. $1/T$ for the three volumes. Although there is some scatter in the points, the straight-line fits are not unreasonable. The best fit parameters are given in Table III. Of particular interest is the parameter E_0, which ranges from 12.7 to 14.9 kcal/mol. From the scatter in the points we estimate that the error in E_0 is ±1.5 kcal/mol.

Table III
Best Fit Parameters E_0 and γ_0 Obtained from Analyzing the Parameter γ from Table I with Eq 23 (See Figure 5)

specific vol, cm^3/g	E_s, kcal/mol	γ_0, s^{-1}
1.012	12.7	1.41×10^{11}
1.022	13.4	7.40×10^{11}
1.032	14.9	1.05×10^{13}

It is tempting to speculate about the origin of this temperature dependence. A process that scatters solitons will contribute to an increase in the soliton velocity relaxation rate, γ. Since γ is Arrhenius with activation energy E_0, it is reasonable to assume that solitons are being scattered by thermal excitations that have a creation energy E_0 and hence a population proportional to $e^{-E_0/kT}$. Acoustic phonon energies, for example, are much less than $E_0 \approx 13$ or 14 kcal/mol, so these phonons could not be responsible for this scattering. Even the highest frequency intramolecular vibration, the C–H stretch, is about 2950 cm^{-1}, corresponding to 8.4 kcal/mol. Other possibilities include thermally created structural defects. One such possibility is the Pechhold kink,[18] a conformationally defective ttgtg'tt sequence. However, modeling studies predict its energy to be about 8 kcal/mol.[4,19,20] Another possibility is the Reneker defect,[21] a very localized 180° buckled twist. Indeed, modeling studies predict its energy to be 13 kcal/mol with an uncertainty of a few kcal/mol,[19,20] corresponding very well with our estimate of $E_0 \approx$ 13–14 kcal/mol. Thus the Reneker defect is a likely candidate for the scattering of solitons. A reasonable question to ask is: If the Reneker defect has a lower energy than the soliton, why is it not *directly* responsible for dielectric relaxation. Presumably, the answer is that because of the very distorted nature of this defect, there exists a sizeable energy barrier to propagation,[22] and hence the defect is relatively immobile. Therefore, even though there are more Reneker defects around than solitons, because of their immobility, they are not as effective in reorienting dipoles as solitons are. One might also wonder why the Pechhold kink is not the major soliton scatterer, since its creation energy is smaller than that of the Reneker defect. The resolution of this question is not understood.

The preceding analysis of the data has been performed without recourse to an underlying model Hamiltonian. However, it is also of interest to analyze the data in terms of the microscopic sine–Gordon model discussed in section 2. Although the sine–Gordon solitons are approximations to the more realistic MB solitons (most importantly, half of the energy of the MB soliton does not arise from the twisted region), it is nevertheless useful to perform the following analysis since we can obtain order-of-magnitude estimates for quantities such as the thermal soliton velocity, the soliton density, and the soliton diffusion constant. These quantities cannot be estimated without a microscopic model.

There are four independent microscopic parameters in the sine–Gordon model (eq 1): the potential barrier A, the moment of inertia I, the spring constant C, and distance between CH_2 units l. The additional parameters—the frequency ω_0, the sound speed c_0, the soliton width α, the soliton mass m^*, and the soliton energy E_s—can all be expressed in terms of the original four. Thus the estimate of *any* four parameters will determine the rest. We take the moment of inertia to be $I = 1.0 \times 10^{-39}$ g cm^2, $l = 1.28$ Å, and $E_s = 18$ kcal/mol. In principle, ω_0 was determined by fitting the experimental data (see Table II), but because of the large extrapolation involved, it is not a reliable choice for the fourth parameter. Thus we will choose α, the soliton width. From comparing the static soliton profile of eq 6 with the MB soliton,[3] we estimate that $\alpha = 2.5l = 3.19$ Å. From these four parameters, the other five can be determined; a list of all the parameters is compiled in Table IV.

Table IV
Estimates of the Appropriate Parameters for the Sine-Gordon Soliton Model

$I = 1.0 \times 10^{-39}$ g cm^2	$c_0 = 5.0 \times 10^5$ cm/s
$l = 1.28 \times 10^{-8}$ cm	$\alpha = 3.19 \times 10^{-8}$ cm
$A = 0.9$ kcal/mol	$m^* = 5.0 \times 10^{-24}$ g
$C = 22.5$ kcal/mol	$E_s = 18$ kcal/mol
$\omega_0 = 1.58 \times 10^{13}$ s^{-1}	

First of all, we note that the value of ω_0 is the same order of magnitude as those determined directly from the experimental fit (see Table II). In addition, $A = 0.9$ kcal/mol, leading to a rotation barrier of $2A \approx 2$ kcal/mol, seems reasonable.[3]

Secondly, since $C \gg A$, the continuum limit, eq 2, is rigorously justified. A typical soliton velocity, v, can be estimated by setting the soliton kinetic energy, $m^*v^2/2$, equal to $kT/2$. For $T = 90$ °C and using m^* above, we obtain $v = 1.0 \times 10^5$ cm/s. Since this is a factor of 5 less than the sound speed c_0, our "nonrelativistic" ($v \ll c_0$) treatment should be adequate. We can also determine the soliton density from eq 11. At $T = 90$ °C, we obtain $n_0 = 3.5 \times 10^{-3}$ cm^{-1}, which is certainly in the dilute limit!

Finally, we note that we can estimate the soliton diffusion constant using the Einstein relation, $D = kT/\zeta = kT/\gamma m^*$. Taking $T = 90$ °C and $\gamma = 4800$ s^{-1} (from Table I, specific volume = 1.022 cm^3/g), we obtain $D = 2.1 \times 10^6$ cm^2/s. Since this is 11 orders of magnitude larger than typical diffusion constants in liquids, we can indeed consider these solitons to be a very mobile species. This extremely large value of D results from a surprisingly small value for γ, the soliton damping constant. While the analysis and interpretation of the experimental data seem to be consistent with the noninteracting soliton model, one should not rule out the possibility that the interaction of solitons with chain folds or with each other is important. This would then modify the long-time behavior of the correlation function. In this case, the analysis of the data in terms of the *noninteracting* model might produce a value for γ that is artificially small, and hence a value for D that is too large.

4. Concluding Remarks

The Brownian soliton model is quite successful in interpreting the experimental data.[1] The agreement of the theoretical fit and the experimental data for the frequency-dependent susceptibility is excellent. Analysis of the temperature dependence of the parameter, B, which is proportional to the soliton density, yields a value for the soliton energy that agrees well with an independent theoretical calculation.[3] From analysis of the temperature dependence of γ, the inverse of the velocity correlation time, we speculate that the soliton friction results from scattering by other thermal defects, most probably the Reneker defect.[21] From our results we can estimate the soliton diffusion constant.

The physical picture that emerges is the following. In thermal equilibrium there exists a very low concentration of topological soliton defects. These solitons are very mobile and cause dielectric relaxation by flipping dipoles as they pass. However, due to scattering with other thermal excitations, these solitons have a finite velocity correlation time, γ^{-1}. The form of the dipole–dipole correlation function or the frequency-dependent susceptibility depends on the ratio of B to γ. When $B \gg \gamma$, one obtains

Debye relaxation, and when $B \ll \gamma$, one obtains a skewed arc for $\chi(\omega)$. As remarked previously, B is the inverse of the time it takes a soliton to arrive at a dipole in the absence of friction. Thus when $B \gg \gamma$, the soliton arrives without having been scattered, while if $B \ll \gamma$, the soliton is scattered many times before it arrives. The first case corresponds to freely streaming solitons, while the latter corresponds to diffusing solitons. B is proportional to the soliton density and thus has an Arrhenius temperature dependence. If we assume that solitons are being scattered by defects, then γ should be proportional to the number of defects and also would have an Arrhenius temperature dependence. Thus both B and γ increase rapidly with increasing temperature. However, since the soliton energy is greater than the defect energy, B increases faster than γ, and therefore Debye behavior is approached at high temperatures. Note however that at the highest experimental temperature $B/\gamma \approx 1$, so soliton scattering is still appreciable.

Skinner and Wolynes[6] originally assumed that solitons are being scattered by phonons and hence the solitons undergo Brownian motion. In this picture solitons lose their velocity correlation gradually as a result of many weak interactions. If, in fact, solitons are being scattered by immobile defects, then a *collisional* model of soliton dynamics is perhaps more appropriate than a Brownian motion picture. In such a model, solitons behave as free particles between collisions. It would be interesting to calculate the dipole–dipole correlation function for solitons undergoing some sort of collisional dynamics and use the results to analyze the present experiments. Such a modification of the Brownian soliton model would be made in the same spirit that Brownian motion theories of rotational relaxation[23] or chemical reactions[24] have been generalized.[25-30]

Acknowledgment. We are grateful to Professor Richard Boyd for sending us experimental data from Dr. J. Sayre's thesis and allowing us to reproduce it here. We thank the National Science Foundation (Grant No. DMR 83-06429) and the donors of the Petroleum Research Fund, administered by the American Chemical Society, for support of this work.

Registry No. Polyethylene (homopolymer), 9002-88-4.

References and Notes

(1) J. A. Sayre, S. R. Swanson, and R. H. Boyd, *J. Polym. Sci. Polym. Phys. Ed.*, **16**, 1739 (1978).
(2) K. S. Cole and R. H. Cole, *J. Chem. Phys.*, **9**, 341 (1941).
(3) M. Mansfield and R. H. Boyd, *J. Polym. Sci., Polym. Phys. Ed.*, **16**, 1227 (1978).
(4) R. H. Boyd, *J. Polym. Sci., Polym. Phys. Ed.*, **13**, 2345 (1975).
(5) M. L. Mansfield, *Chem. Phys. Lett.*, **69**, 383 (1980).
(6) J. L. Skinner and P. G. Wolynes, *J. Chem. Phys.*, **73**, 4015, 4022 (1980).
(7) See, for example, "Solutions in Condensed Matter Physics", A. R. Bishop and T. Schneider, Eds., Springer-Verlag, New York, 1978.
(8) G. Williams, *Chem. Rev.*, **72**, 55 (1972).
(9) M. A. Collins, A. Blumen, J. F. Currie, and J. Ross, *Phys. Rev. B*, **19**, 3630 (1979).
(10) Y. Wada and J. R. Schrieffer, *Phys. Rev. B*, **18**, 3897 (1978); Y. Wada and H. Ishiuchi, *J. Phys. Soc. Jpn.*, **51**, 1372 (1981).
(11) P. S. Sahni and G. F. Mazenko, *Phys. Rev. B*, **20**, 4674 (1979).
(12) G. Williams and D. C. Watts, *Trans. Faraday Soc.*, **66**, 80 (1970).
(13) M. Abramowitz and I. A. Stegun, Eds., "Handbook of Mathematical Functions", Dover, New York, 1972.
(14) D. W. Davidson and R. H. Cole, *J. Chem. Phys.*, **19**, 1484 (1951).
(15) C. P. Lindsey and G. D. Patterson, *J. Chem. Phys.*, **73**, 3348 (1980).
(16) J. A. Sayre, Ph.D. Dissertation, University of Utah, 1977.
(17) The data for $\epsilon''(\omega)$ did not approach the base line on either side of the α-relaxation peak but rather rose again. Thus, data points out in the wings included contributions from other relaxation peaks. Since we are only interested in the main peak, we did not use those points that reflected a significant contribution from other peaks (based on our best estimate).
(18) W. Pechhold, S. Blasenbrey, and S. Woerner, *Colloid Polym. Sci.*, **189**, 14 (1963).
(19) R. H. Boyd and J. A. Sayre, *J. Polym. Sci., Polym. Phys. Ed.*, **17**, 1627 (1979).
(20) H. Sherr, P. C. Hagele, and H. P. Grossman, *Colloid Polym. Sci.*, **252**, 871 (1974).
(21) D. H. Reneker, *J. Polym. Sci.*, **59**, 539 (1962).
(22) D. H. Reneker, B. M. Fanconi, and J. Mazur, *J. Appl. Phys.*, **48**, 4032 (1977).
(23) M. Fixman and K. Rider, *J. Chem. Phys.*, **51**, 2425 (1969).
(24) H. A. Kramers, *Physica*, **7**, 284 (1940).
(25) R. G. Gordon, *J. Chem. Phys.*, **44**, 1830 (1966).
(26) G. T. Evans, *Chem. Phys. Lett.*, **57**, 113 (1978).
(27) J. L. Skinner and P. G. Wolynes, *J. Chem. Phys.*, **69**, 2143 (1978); **72**, 4913 (1980); *Physica A (Amsterdam)*, **96**, 561 (1979); D. K. Garrity and J. L. Skinner, *Chem. Phys. Lett.*, **95**, 46 (1983).
(28) J. A. Montgomery, Jr., D. Chandler, and B. J. Berne, *J. Chem. Phys.*, **70**, 4056 (1979).
(29) J. T. Hynes, *Chem. Phys. Lett.*, **79**, 344 (1981).
(30) G. T. Evans, *J. Chem. Phys.*, **78**, 4963 (1983).